

A New Class of Photo-Cross-Linkable Side Chain Liquid Crystalline Polymers Containing Bis(benzylidene)cyclohexanone Units

Gangadhara and Kaushal Kishore*

Department of Inorganic and Physical Chemistry, Indian Institute of Science, Bangalore 560 012, India

Received April 29, 1994; Revised Manuscript Received October 13, 1994*

ABSTRACT: This paper reports a new class of photo-cross-linkable side chain liquid crystalline polymers (PSCLCPs) based on the bis(benzylidene)cyclohexanone unit, which functions as both a mesogen and a photoactive center. Polymers with the bis(benzylidene)cyclohexanone unit and varying spacer length have been synthesized. Copolymers of bis(benzylidene)cyclohexanone containing monomer and cholesterol benzoate containing monomer with different compositions have also been prepared. All these polymers have been structurally characterized by spectroscopic techniques. Thermal transitions were studied by DSC, and mesophases were identified by polarized light optical microscopy (POM). The intermediate compounds OH- x , the monomers SCLCM- x , and the corresponding polymers PSCLCP- x , which are essentially based on bis(benzylidene)cyclohexanone, all show a nematic mesophase. Transition temperatures were observed to decrease with increasing spacer length. The copolymers with varying compositions exhibit a cholesteric mesophase, and the transition temperatures increase with the cholesteric benzoate units in the copolymer. Photolysis of the low molecular weight liquid crystalline bis(benzylidene)cyclohexanone compound reveals that there are two kinds of photoreactions in these systems: the *EZ* photoisomerization and $2\pi + 2\pi$ addition. The *EZ* photoisomerization in the LC phase disrupts the parallel stacking of the mesogens, resulting in the transition from the LC phase to the isotropic phase. The photoreaction involving the $2\pi + 2\pi$ addition of the bis(benzylidene)cyclohexanone units in the polymer results in the cross-linking of the chains. The liquid crystalline induced circular dichroism (LCICD) studies of the cholesterol benzoate copolymers revealed that the cholesteric supramolecular order remains even after the photo-cross-linking.

Introduction

Liquid crystalline polymers (LCPs) have attracted considerable interest in recent years due to the unique combination of the polymer-specific properties and anisotropic behavior of liquid crystals (LCs).¹⁻⁵ Among these polymers, photo-cross-linkable LCPs have generated special attention as they have both mesogens and photoactive groups in their structure.⁶⁻¹⁰ The former incorporates LC properties to the polymer and the later facilitates cross-linking of the chains under the influence of UV or visible radiation. This class of polymers is useful in fabricating anisotropic networks and thin films,⁷ information storage devices,^{11,12} nonlinear optical devices,^{13,14} aligned membranes for permeation of gases and drugs, etc.^{15,16} The photochemistry of these polymers is interesting from topochemical aspects since the photoreactions take place in ordered LC media.^{17,18} All the photo-cross-linkable LCPs reported so far contain the cinnamate ester group as a photoactive center, which undergoes photodimerization on irradiation leading to the cross-linking of the polymer chains.¹⁹⁻²¹ We have recently studied a new class of photo-cross-linkable main chain LCPs which contain bis(benzylidene)cycloalkane units.²²

Among the two major classes of LCPs, namely, the main chain LCPs and the side chain LCPs, the latter exhibit lower transition temperatures and tend to harden into a glassy state with the retention of LC order when cooled from the LC state. Besides, the side chain LCPs have good solubility in common organic solvents, display a rich variety of LC phases such as S_A^* and S_C^* , and exhibit quick response to an external field due to their low melt viscosity. Hence, side chain LCPs are

widely studied for applications in electronic and optical devices.²³ In this paper we present a new class of photo-cross-linkable side chain liquid crystalline polymers (PSCLCPs) based on the bis(benzylidene)cycloalkane unit.

The bis(benzylidene)cycloalkane unit can exist in three isomeric structures (Figure 1). The *EE* isomer among these has a linear rodlike shape which fulfills the requirement of geometrical anisotropy necessary for the molecule to be a mesogen. The α,β -unsaturated ketone functionality of the bis(benzylidene)cycloalkane has the capacity to undergo photoisomerization,^{24,25} photodimerization,²⁶⁻²⁹ and photopolymerization³⁰ reactions. The latter two reactions in the polymer can lead to the cross-linking of the chains. The present study includes the synthesis, structural characterization, liquid crystalline property, and photo-cross-linking behavior of the polymers containing *EE*-bis(benzylidene)cyclohexanone groups pendent to the polymethacrylate backbone. Using the above mesogen, we have attempted to synthesize photo-cross-linkable cholesteric side chain liquid crystalline polymers and to freeze-in the helicoidal conformation by cross-linking. Such cholesteric networks are of interest in passive optical devices.³¹⁻³³

Experimental Section

p-Hydroxybenzaldehyde (Merck-Schuchart), *p*-anisaldehyde (Sisco Chemicals Ltd.), *p*-hydroxybenzoic acid (BDH Chemicals Ltd.), methacrylic acid (Spectrochem Ltd.), methacryloyl chloride (Fluka AG), 1,6-hexanediol (Fluka AG), 1,8-octanediol (Merck-Schuchart), chloroethanol (BDH Chemicals Ltd.), and cholesterol (Koch-light Laboratories Ltd.) were used as received. AIBN (Koch-light Laboratories Ltd.) was recrystallized twice from methanol. Cyclohexanone (Glaxo Laboratories) and all the solvents were purified by distillation.

* Abstract published in *Advance ACS Abstracts*, December 15, 1994.

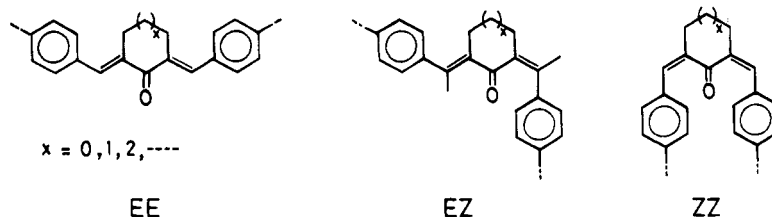


Figure 1. Isomeric structures of bis(benzylidene)cycloalkanones.

Synthesis. 4-Bromo-1-butanol was prepared from tetrahydrofuran.³⁴ 6-Bromo-1-hexanol and 8-bromo-1-octanol were synthesized from the respective diols using 48% HBr.³⁵

2-(4-Methoxybenzylidene)cyclohexanone. This compound was prepared by refluxing a mixture of 58.9 g (0.6 mol) of cyclohexanone and 27.2 g (0.2 mol) of *p*-anisaldehyde in 150 mL of 1 N NaOH solution for 3 h. The oily layer at the bottom was separated and crystallized from hexane: yield 36 g (83%); mp 72 °C. IR (KBr): 1674 ($\nu_{C=O}$), 1581 cm^{-1} ($\nu_{C=C}$, exocyclic). ¹H NMR (CDCl_3 , TMS): δ 1.8–1.7 (2m, 4H, $\text{CH}_2\text{CH}_2\text{CH}_2$), 2.41 (t, 2H, COCH_2CH_2), 2.72 (t, 2H, $=\text{CH}_2\text{CH}_2$), 3.71 (s, 3H, ArOCH_3), 6.91 (d, 2H, aromatic), 7.29 (d, 2H, aromatic), 7.41 (s, 1H, $>\text{CCH}=\text{Ar}$).

4-(ω -Hydroxyalkyl-1-oxy)benzaldehyde (CHO- x , $x = 2, 4, 6$, and 8). These compounds were prepared by the etherification of *p*-hydroxybenzaldehyde with the corresponding ω -halo alcohols in dimethylformamide (DMF) in the presence of anhydrous potassium carbonate. A typical example of the synthesis of 4-(6-hydroxyhexyl-1-oxy)benzaldehyde is outlined below.

p-Hydroxybenzaldehyde (18.5 g (0.15 mol)) was dissolved in 100 mL of dry DMF to which 20.0 g (0.15 mol) of anhydrous potassium carbonate was added in one lot. The mixture was stirred at 80 °C for 15 min and cooled to room temperature. Then 29.0 g (0.16 mol) of 6-bromo-1-hexanol was added dropwise over 30 min, and the mixture was heated again to 80 °C with stirring for 6 h. The reaction mixture was cooled and poured into 500 mL of ice cold water. The product was extracted with ether, washed twice with 5% aqueous NaOH and twice with water, and dried over anhydrous Na_2SO_4 overnight. The 4-(6-hydroxyhexyl-1-oxy)benzaldehyde was isolated as an oily substance by evaporating the ether; yield 21.3 g (64%). IR (KBr): 3406 (ν_{O-H}), 1668 cm^{-1} ($\nu_{C=O}$). ¹H NMR (CDCl_3 , TMS): δ 1.58 (m, 2H, $\text{CH}_2\text{CH}_2\text{OH}$), 1.77 (m, 2H, $\text{CH}_2\text{CH}_2\text{OAr}$), 3.46 (t, 2H, $\text{CH}_2\text{CH}_2\text{OH}$), 3.98 (t, 2H, $\text{CH}_2\text{CH}_2\text{OAr}$), 6.90 (d, 2H, aromatic), 7.76 (d, 2H, aromatic), 9.80 (s, 1H, ArCHO).

2-[4-(ω -Hydroxyalkyl-1-oxy)benzylidene]-6-[4-methoxybenzylidene]cyclohexanone (OH- x , $x = 2, 4, 6$, and 8). These compounds were prepared by the reaction of equimolar amounts of 4-(ω -hydroxyalkyl-1-oxy)benzaldehyde and 2-(4-methoxybenzylidene)cyclohexanone in ethanolic NaOH solution. A typical procedure for the preparation of 2-[4-(6-hydroxyhexyl-1-oxy)benzylidene]-6-[4-methoxybenzylidene]cyclohexanone is given below.

4-(6-Hydroxyhexyl-1-oxy)benzaldehyde (5 g (0.023 mol)) and 5.5 g (0.023 mol) of 2-(4-methoxybenzylidene)cyclohexanone were dissolved in 20 mL of ethanol, and 1 g of NaOH was added in small quantities with stirring for about 15 min. The stirring was continued for 24 h; during this period the product precipitated out as a yellow solid which was separated by filtration and recrystallized from ethanol–water mixture (80/20 v/v); yield 7.6 g (76%). IR (KBr): 1661 ($\nu_{C=O}$), 1599 ($\nu_{C=C}$ exocyclic), 3420 cm^{-1} (ν_{O-H}). ¹H NMR (CDCl_3 , TMS): δ 1.7–2.0 (m, 10H, $\text{CH}_2\text{CH}_2\text{CH}_2$), 2.89 (s, br, 4H, CCH_2CH_2), 3.64 (t, 2H, $\text{CH}_2\text{CH}_2\text{OH}$), 3.89 (s, 3H, ArOCH_3), 3.96 (t, 2H, $\text{CH}_2\text{CH}_2\text{OAr}$), 6.9–7.5 (2m, 8H, aromatic), 7.74 (s, 2H, $>\text{C}=\text{CHAr}$).

2-[4-(ω -(Methacryloyloxy)alkyl-1-oxy)benzylidene]-6-[4-methoxybenzylidene]cyclohexanone (SCLCM- x , $x = 2, 4, 6$, and 8). All the monomers were synthesized by a similar procedure involving the esterification of 2-[4-(ω -hydroxyalkyl-1-oxy)benzylidene]-6-[4-methoxybenzylidene]cyclohexanone using methacryloyl chloride. A typical procedure is given here. 2-[4-(2-Hydroxyethyl-1-oxy)benzylidene]-6-[4-methoxybenzylidene]cyclohexanone (1.5 g (4.12×10^{-3} mol))

was dissolved in 50 mL of dry dichloromethane to which 3 mL (0.04 mol) of dry triethylamine (TEA) was added. The solution was then cooled to 0 °C and 0.45 g (4.3×10^{-3} mol) of methacryloyl chloride was added dropwise. The resulting mixture was stirred at room temperature for about 24 h and subsequently diluted with 50 mL of dichloromethane. The solution was washed first with 25 mL of 5% HCl, then twice with 5% NaOH, and finally with cold water and dried over anhydrous Na_2SO_4 . The solvent was removed at room temperature to yield 1.69 g (91%) of the yellow product. IR (KBr): 1715 ($\nu_{C=O}$, ester), 1662 ($\nu_{C=O}$, ketonic), 1599 cm^{-1} ($\nu_{C=C}$). ¹H NMR (CDCl_3 , TMS): δ 1.54 (s, 3H, $\text{CH}_2=\text{CCH}_3$), 3.85 (s, 3H, CH_3OAr), 4.25 (t, 2H, $\text{CH}_2\text{CH}_2\text{OAr}$), 4.59 (t, 2H, $\text{CH}_2\text{CH}_2\text{OCO}$), 5.5–6.2 (2s, 2H, $\text{CH}_2=\text{C}(\text{CH}_3)$), 6.9–7.5 (2m, 8H, aromatic), 7.76 (s, 2H, $>\text{C}=\text{CHAr}$). To achieve higher purity, the monomers were purified by column chromatography (silica gel, ethyl acetate/hexane (20/80 v/v) eluent).

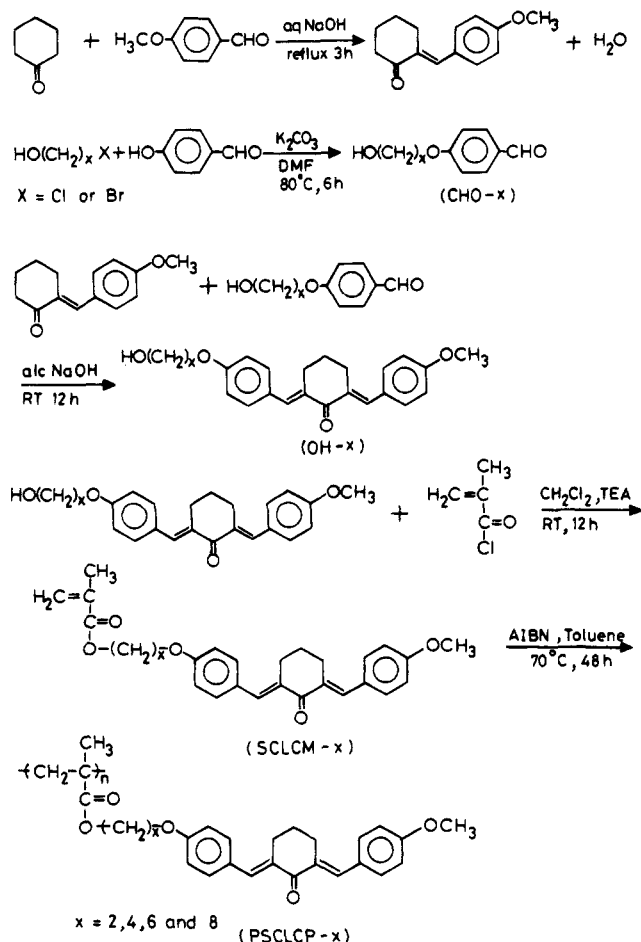
4-(6-Hydroxyhexyl-1-oxy)benzoic Acid. *p*-Hydroxybenzoic acid (8.9 g (0.05 mol)) was dissolved in 15 mL of ethanol, and KOH (6.2 g (0.11 mol)) in 10 mL of water was added. A trace of KI was added as a catalyst and the mixture was refluxed. During refluxing 11.0 g (0.06 mol) of 6-bromo-1-hexanol was added dropwise over 3 h. Subsequently the reaction mixture was refluxed for 12 h and ethanol was distilled off at the end of the reaction. The remaining solution was then diluted with 50 mL of cold water, washed with ether, and strongly acidified with HCl. The product, separated as a white solid, was collected and washed several times with water. Further purification was done by recrystallization from acetone–water mixture (75:25): yield 9.5 g (79%); mp 139 °C. IR (KBr): 3328 (ν_{O-H}), 1671 cm^{-1} ($\nu_{C=O}$). ¹H NMR (CDCl_3 , TMS): δ 1.3–1.8 (m, 8H, $\text{CH}_2\text{CH}_2\text{CH}_2$), 3.51 (t, 2H, $\text{ArOCH}_2\text{CH}_2$), 3.91 (t, 2H, $\text{CH}_2\text{CH}_2\text{OH}$), 6.8–7.9 (2d, 4H, aromatic).

4-[6-(Methacryloyloxy)hexyl-1-oxy]benzoic Acid. 4-(6-Hydroxyhexyl-1-oxy)benzoic acid (7.5 g (0.03 mol)), 0.5 g of hydroquinone, 0.5 g of *p*-toluenesulfonic acid, and 0.1 g of boric acid were added to a mixture of 50 mL of benzene and 25 g (0.3 mol) of methacrylic acid. The mixture was refluxed for 72 h and water formed was removed by azeotropic distillation. The reaction mixture was then cooled and mixed thoroughly with 200 mL of ether. The ether layer was separated, washed several times with water, and dried over anhydrous Na_2SO_4 . The product was isolated as a white solid by evaporating the ether; yield 8.31 g (85%). IR (KBr): 3500 (ν_{O-H}), 1716 ($\nu_{C=O}$, ester), 1688 cm^{-1} ($\nu_{C=O}$, acid). ¹H NMR (CDCl_3 , TMS): δ 1.5–1.9 (m, 8H, $\text{CH}_2\text{CH}_2\text{CH}_2$), 1.91 (s, 3H, $=\text{C}(\text{CH}_3)\text{COO}$), 4.01 (t, 2H, $\text{ArOCH}_2\text{CH}_2$), 4.13 (t, 2H, $\text{CH}_2\text{CH}_2\text{COO}$), 5.5–6.1 (2s, 2H, $\text{CH}_2=\text{C}(\text{CH}_3)$), 6.9–8.1 (2d, 4H, aromatic).

4-[6-(Methacryloyloxy)hexyl-1-oxy]benzoyl Chloride. 4-[6-(Methacryloyloxy)hexyl-1-oxy]benzoic acid (6.5 g (0.02 mol)) was dissolved in 25 mL of dry dichloromethane. To this solution were added 6.4 g (0.05 mol) of oxalyl chloride dropwise and a drop of pyridine as a catalyst. The reaction mixture was then stirred at room temperature for 12 h. The product was isolated by evaporating the dichloromethane and excess of oxalyl chloride under vacuum at 40 °C; yield 6.6 g (98%). ¹H NMR (CDCl_3 , TMS): δ 1.5–1.8 (m, 8H, $\text{CH}_2\text{CH}_2\text{CH}_2$), 1.84 (s, 3H, $\text{C}(\text{CH}_3)\text{COO}$), 3.9 (t, 2H, $\text{ArOCH}_2\text{CH}_2$), 4.1 (t, 2H, $\text{CH}_2\text{CH}_2\text{COCl}$), 5.5–6.1 (2s, 2H, $\text{CH}_2=\text{C}(\text{CH}_3)\text{COO}$), 6.9–8.1 (2d, 4H, aromatic).

Cholesteryl 4-[6-(Methacryloyloxy)hexyl-1-oxy]benzoate. Cholesterol (3.9 g (0.01 mol)) was dissolved in 15 mL of dry dichloromethane containing 3.9 mL (0.03 mol) of triethylamine, and the mixture was cooled to 0 °C. To this mixture was added dropwise a solution of 3.4 g (0.01 mol) of

Scheme 1

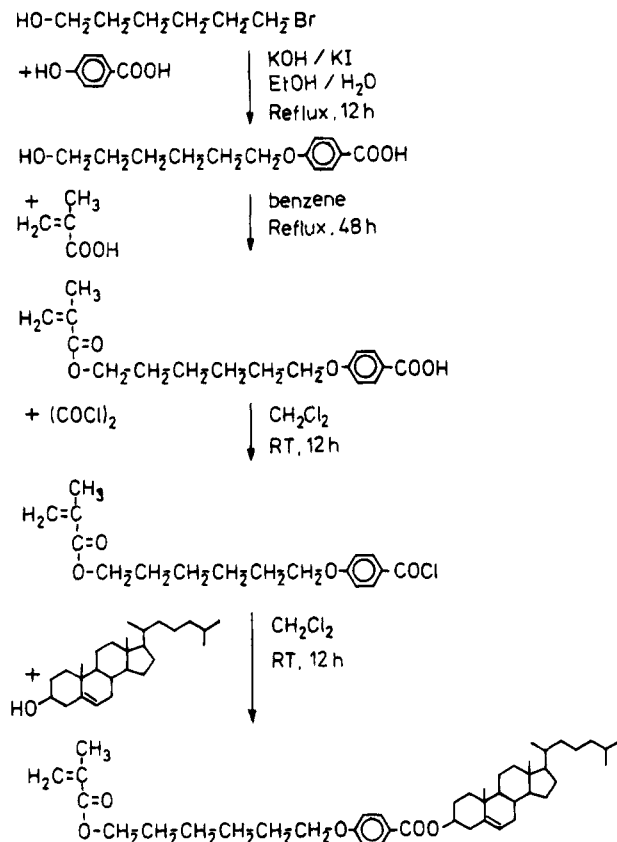


4-[6-(methacryloyloxy)hexyl-1-oxy]benzoyl chloride in 10 mL of dichloromethane for 1 h. After completion of the addition, the reaction mixture was stirred at room temperature for 12 h and then diluted with 100 mL of ether. The ether layer was then washed with 10% HCl till the aqueous layer remained acidic; subsequently it was washed twice with 10% NaOH solution and twice with distilled water. The ether solution was then dried over anhydrous Na_2SO_4 , and evaporation of ether gave the title compound. Further purification was done by passing through a silica gel column using a 20:80 (v/v) mixture of ethyl acetate and hexane as the eluent; yield 6.2 g (90%). IR (KBr): 1713 cm^{-1} ($\nu_{\text{C=O}}$). ^1H NMR (CDCl_3 , TMS): δ 0.7–2.1 (m, 43H, CH_2 and CH_3), 3.96 (t, 2H, $\text{ArOCH}_2\text{CH}_2$), 4.18 (t, 2H, $\text{CH}_2\text{CH}_2\text{CH}_2$), 4.80 (m, 1H, OOCCH<), 5.38 (d, 1H, $>\text{C}=\text{CHCH}_2$), 5.5–6.1 (2s, 2H, $\text{CH}_2=\text{C}(\text{CH}_3)\text{COO}$), 6.8–8.0 (2d, 4H, aromatic).

Radical Polymerization. The homopolymerization and copolymerization of the monomers were carried out using AIBN as the initiator. For example, 300 mg of SCLCM-2 and 3 mg (1 wt % of the monomer) of AIBN were taken in a glass ampule and dissolved in 1.5 mL of dry toluene. The solution was degassed by several freeze–pump–thaw cycles under vacuum and sealed. The ampule was then kept at 70°C for 48 h; subsequently it was opened and the contents were poured into 50 mL of methanol. The precipitated solid was separated by filtration and purified by repeated precipitation from chloroform into methanol.

Measurements. The molecular weights were determined with a Waters GPC in toluene solution, and polystyrene standards were used for calibration. ^1H NMR spectra were recorded on a 400 MHz Bruker AMX-400 FTNMR spectrometer. The chemical shifts were calibrated from tetramethylsilane (TMS). Infrared spectra were recorded on a Bio-Rad FTS 7 FTIR spectrophotometer using KBr pellets. The UV–visible absorption spectra were recorded on a Hitachi U-3400 spectrophotometer. A DuPont TA9900 differential scanning

Scheme 2



calorimeter (DSC) was used to determine the thermal transitions. The glass transition temperature (T_g) was taken as the middle point of the heat capacity change. All heating and cooling rates were $10^\circ\text{C}/\text{min}$, and the sample weight was 30 mg. A Leitz Model BK-2, optical polarized microscope equipped with a hot stage was used to observe the thermal transitions and to analyze the anisotropic textures. CD spectra were run on a JASCO J500 spectrometer calibrated with 0.10% camphorsulfonic acid- d_{10} .

The photolysis of the polymers was done in solution as well as in films. For UV–visible spectral studies, films were cast from the chloroform solution over the outer surface of a 1 cm quartz cuvette. For the FTIR measurements, a thin film of polymer was formed on one side of a KBr pellet of 10 mm diameter and 0.5 mm thickness. The film thickness was adjusted to get the absorbance between 0.05 and 0.10. The photochemical studies were carried out in a discontinuous mode; i.e., the samples were exposed to UV radiation from a 125 W medium-pressure mercury lamp, kept at a distance of 10 cm from the sample for varying intervals of time. The irradiated films were subsequently subjected to spectral analysis.

Results and Discussion

Synthesis. The synthetic routes for the bis(benzylidene)cyclohexanone-based monomers and polymers are shown in Scheme 1. First, the monobenzylidene was prepared by reacting *p*-anisaldehyde with a 3 mol excess of cyclohexanone. It was subsequently converted to bisbenzylidene by reacting with an equimolar quantity of (ω -hydroxyalkyloxy)benzaldehyde. The polymerizable methacrylate moiety was then linked to the bisbenzylidene unit by reacting with methacryloyl chloride. The cholesteric benzoate based monomer was synthesized according to Scheme 2. The resulting monomers were free radically polymerized using 1 wt % of AIBN initiator in toluene at 70°C . The yield and molecular weight are given in Table 1. The polymers were

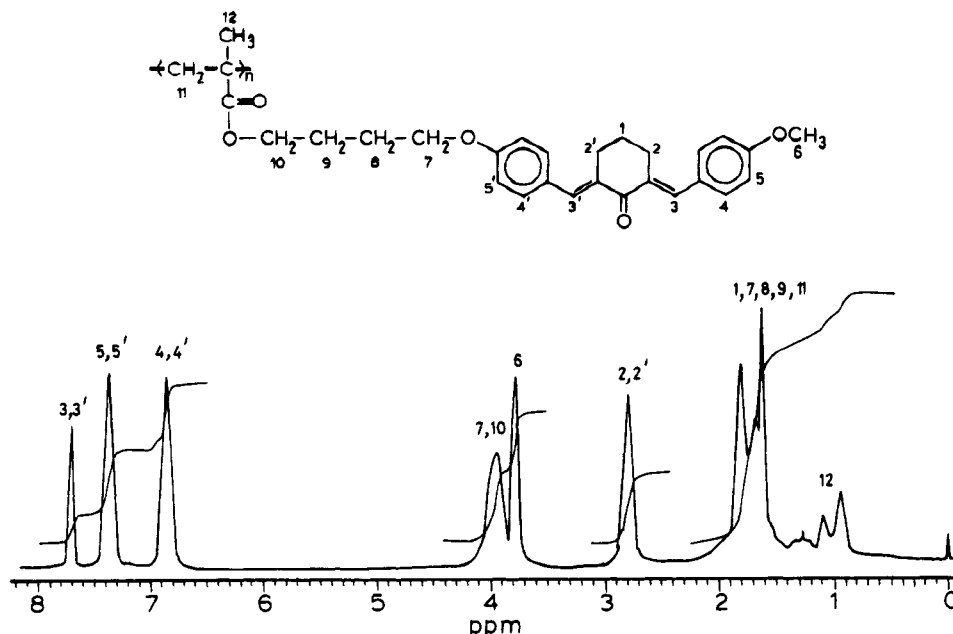


Figure 2. Representative 400 MHz ^1H NMR spectrum of PSCLCP-4 in CDCl_3 .

Scheme 3

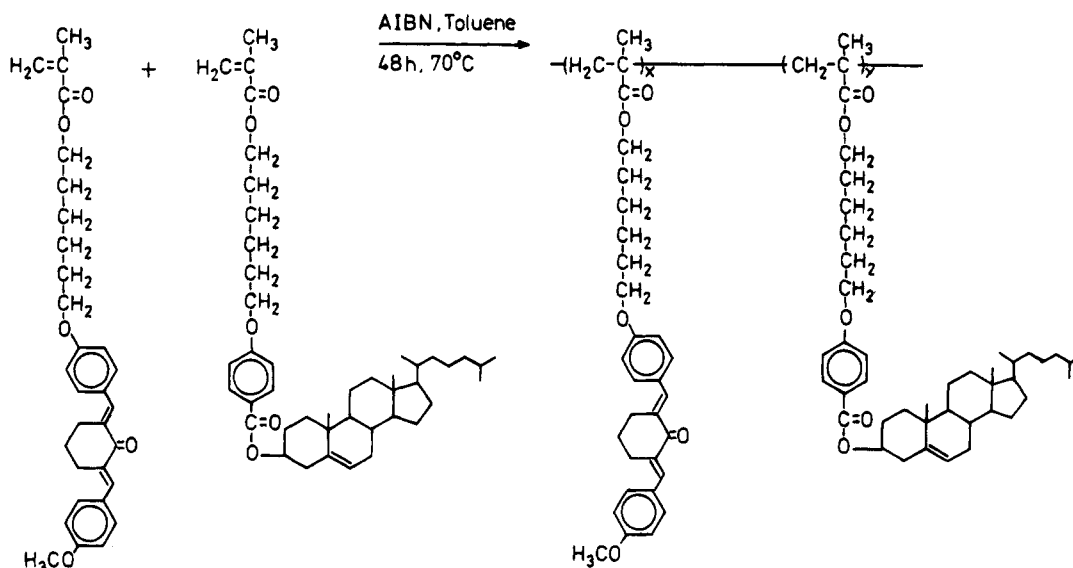


Table 1. Yields, Molecular Weights, and Thermal Transition Temperatures for the Polymers PSCLCP- x

polymer	yield (%)	mol wt		PD ^a	transition temp (°C)			
		\bar{M}_n	\bar{M}_w		heating ^b		cooling ^c	
					T_g	T_i	T_g	T_i
PSCLCP-2	67	31 000	67 000	2.17	100.8	154.8	83.3	148.0
PSCLCP-4	61	29 000	70 000	2.40	75.0	144.1	67.1	125.0
PSCLCP-6	69	36 000	60 000	1.65	50.0	148.0	50.0	148.0
PSCLCP-8	79	38 000	78 000	2.05	45.6	139.1	36.9	128.6

^a Polydispersity. ^b Taken from second heating scan. ^c Taken from first cooling scan.

structurally characterized by UV-visible, IR, and NMR spectroscopic techniques. A typical ^1H NMR spectrum for PSCLCP-4 is given in Figure 2. The copolymerizations were carried out by taking two monomers based respectively on bis(benzylidene)cyclohexanone and cholesteryl benzoate with a hexamethylene spacer in various feed ratios (Scheme 3). The copolymer compositions were determined from the ^1H NMR spectra, and the results are displayed in Table 2. All the polymers with bis(benzylidene)cyclohexanone units were yellow and

Table 2. Copolymer Compositions, Yields, Molecular Weights, and Thermal Transition Temperatures for the Copolymers

copolymer	m_{feed}^a	m_{polymer}^b	yield (%)	transition temp (°C)			
				heating scan ^c		cooling scan ^d	
				T_g	T_i	T_g	T_i
COP-1	8	28	62	48.7	150.0	37.2	140.4
COP-2	15	29	65	52.0	164.6	40.2	159.2
COP-3	25	35	74	56.0	173.2	40.0	154.0
COP-4	50	64	78	70.0	206.2	51.3	^e
COP-5	100	100	86	85.0	273.0		^f

^a Percentage of cholesteryl benzoate monomer in the feed. ^b Percentage of cholesteryl benzoate unit in the polymer. ^c For COP-4 and COP-5 values are taken from the first heating scan and for the remaining samples from the second heating scan. ^d Taken from the first DSC cooling scan. ^e Exotherm was not clearly visible in the thermogram. ^f Sample degrades at the isotropic phase during the first DSC heating scan.

were stored in the dark below 10 °C. We also attempted to synthesize polymers with an acrylate instead of a methacrylate backbone, but the yield was very low and

Table 3. Temperatures (°C) and Enthalpies (J/g) of Thermal Transitions^a for 2-[4-(ω -Hydroxyalkyl-1-oxy)benzylidene]-6-[4-methoxybenzylidene]cyclohexanone (OH- x)

OH- x	T_g	T_c^b	ΔH_c	T_m	ΔH_m	T_i	ΔH_i
OH-2				144	62.2	164	0.6
OH-4	5	48	6.5	130	25.7	152	0.4
OH-6	4	58	18.4	69	10.4	149	2.3
OH-8	-2	83	19.6	100	6.6	127	3.2

^a From the second DSC heating scan. ^b Crystal to crystal transition temperature.

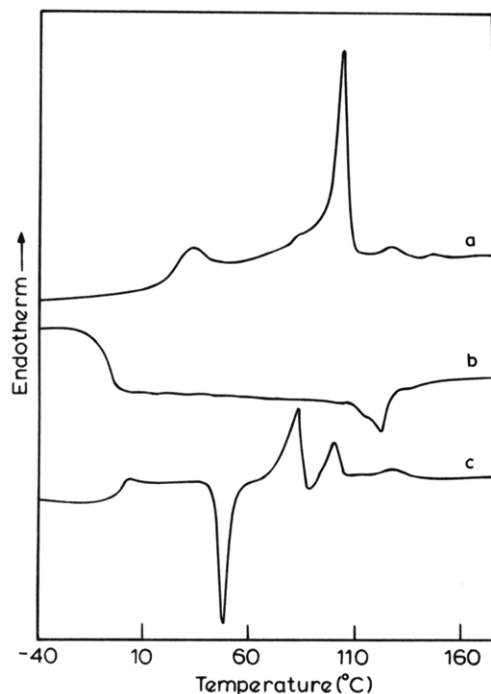


Figure 3. DSC thermograms for OH-8: (a) first heating scan; (b) first cooling scan; (c) second heating scan.

the polymers formed were cross-linked, probably due to the attack of highly reactive acrylate radicals on the benzylidene exocyclic double bonds.

Liquid Crystalline Properties. The mesogenic transitions were studied by DSC and POM. It has been confirmed that the intermediate compounds OH- x , monomers SCLCM- x , and polymers PSCLCP- x all show LC properties. Generally in the DSC thermogram, at the highest transition temperature there was a single endotherm corresponding to the transition from the LC phase to the isotropic phase. The transition in some cases from crystal to LC was marked by more than one endotherm. When such multiple peaks were observed, the one having the highest temperature was attributed to the crystal to mesophase transition. The POM studies show no evidence of fluidity below this temperature. Lower transition peaks were assigned to unidentified crystal to crystal transformations.^{36,37} Transitions in a few of the low molecular weight LCs showed a large dependence on the thermal history of the sample. Annealing at a temperature between T_g and T_m seems to be essential for observing the transitions clearly in such cases.

2-[4-(ω -Hydroxyalkyl-1-oxy)benzylidene]-6-[4-methoxybenzylidene]cyclohexanone (OH- x , $x = 2, 4, 6$, and 8). All four compounds show a nematic mesophase. The transition temperatures and enthalpies of transition are given in Table 3. Figure 3 shows a representative DSC thermogram for OH-8. In the first

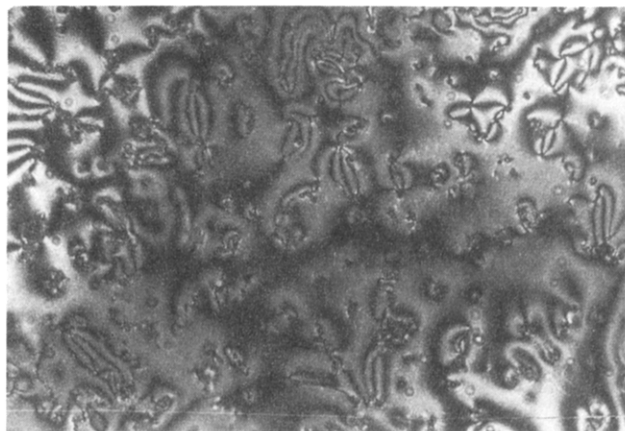


Figure 4. Optical polarization microphotograph of OH-8 at 105 °C.

Table 4. Thermal Transition Temperatures (°C) and Enthalpies of Transition (J/g)^a for 2-[4-(ω -(Methacryloyloxy)alkyl-1-oxy)benzylidene]-6-[4-methoxybenzylidene]cyclohexanone (SCLCM- x)

SCLCM- x	T_g	T_c	ΔH_c	T_m	ΔH_m	T_i	ΔH_i
SCLCM-2	7	37	2.3	66	34.5		
SCLCM-4	-7	15	3.8	60	16.0	99	1.5
SCLCM-6	-10	8	3.2	54	12.6	80	0.8
SCLCM-8	-17	24	2.7	48	43.3	91	0.5

^a Values have been taken from the second DSC heating scan.

heating scan (curve a), a small endotherm at 32 °C was assigned for the crystal to crystal transition, which is followed by an endotherm at 103 °C for the melting of the crystal to the LC phase. The isotropization endotherm appears at 129 °C. On cooling from the isotropic melt (curve b), the nematic phase appears as an exotherm at 121 °C. The display of the nematic phase exhibited by this compound was confirmed by POM observations (Figure 4). On further cooling, the nematic melt freezes at T_g (-8 °C) into an amorphous glassy state with the retention of the LC order and no crystallization was observed. Interestingly, in the second heating scan (curve c), after the T_g at -2 °C, an exotherm at 49 °C was observed for the crystallization. The crystallites thus formed show multiple endotherms at 89 and 100 °C for melting to the nematic phase. The endotherm at 127 °C corresponds to the nematic to isotropic transition. These observations were found to be reproducible for the successive heating cycles.

From the thermal data given in Table 3, it can be inferred that all the compounds, except OH-2, showed multiple endotherms for melting. The nematic to isotropic transition temperature and the corresponding enthalpy of transition decrease with increasing spacer length. On cooling from the isotropic phase, with increasing spacer length, the compounds show a greater tendency to solidify into the LC glassy state.

2-[4-(ω -(Methacryloyloxy)alkyl-1-oxy)benzylidene]-6-[4-methoxybenzylidene]cyclohexanone (SCLCM- x , $x = 2, 4, 6$, and 8). Among the four monomers, the one with two methylene units in the spacer (SCLCM-2) did not exhibit mesomorphic behavior. Table 4 shows the temperatures and enthalpies of transition for these monomers. Figure 5 shows the DSC heating and cooling traces for SCLCM-8. The first heating scan (curve a) showed an endotherm at 72 °C with a shoulder at 52 °C for the melting to the nematic phase. This is followed by a small endotherm at 91 °C for the nematic to isotropic transition. No clear transi-

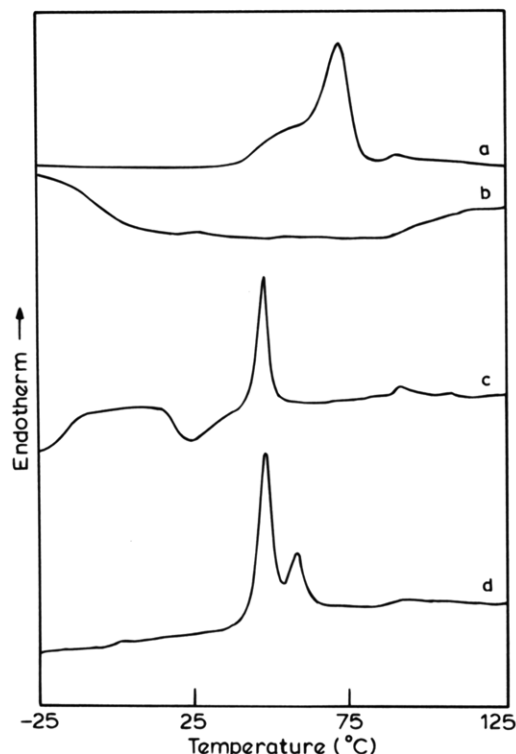


Figure 5. DSC thermograms for SCLCM-8: (a) first heating scan; (b) first cooling scan; (c) second heating scan; (d) heating scan of the annealed sample (25 °C, 24 h).



Figure 6. Optical polarization microphotograph of SCLCM-8 at 60 °C.

tion peaks, except T_g at -19 °C, were seen on cooling from the isotropic state (curve b). However, in POM studies, the isotropic to nematic transition on cooling was observed at 84 °C. The crystallization exotherm during the second heating scan (curve c) appeared at 24 °C after the T_g at -17 °C. The newly formed crystallites then melt into a nematic fluid at 48 °C and on further heating change over to an isotropic liquid at 91 °C. The crystallization can also be induced by annealing between T_g and T_m . The heating thermogram (curve d) of the annealed sample, therefore, did not show the crystallization but a melting transition was seen. These monomers also exhibit a nematic mesophase as depicted in Figure 6.

The thermal data given in Table 4 demonstrate that both T_g and T_m decrease with increasing spacer length. All the monomers failed to crystallize during the DSC cooling. However, crystallization did occur in the subsequent heating cycle. Transition temperatures of

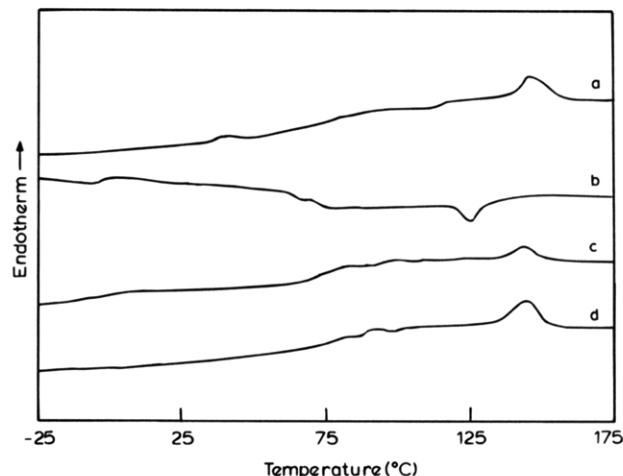


Figure 7. DSC thermograms for PSCLCP-8: (a) first heating scan; (b) first cooling scan; (c) second heating scan; (d) heating scan of the annealed sample (80 °C, 24 h).

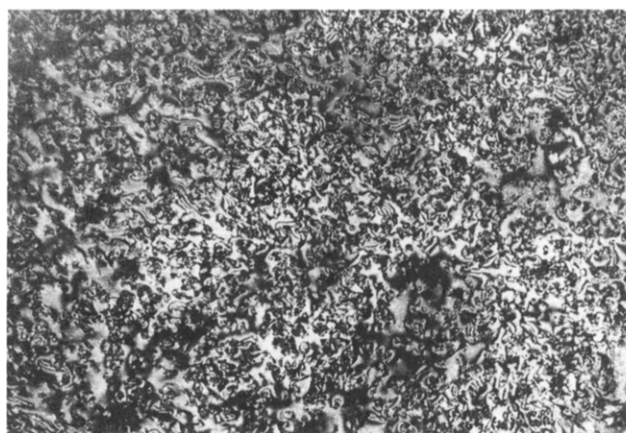


Figure 8. Optical polarization microphotograph of PSCLCP-6 at 130 °C.

OH- x (Table 3) were higher than those of the corresponding SCLCM- x , probably due to the hydrogen bonding between the hydroxy groups in the former.

Polymers. All the polymers exhibit LC properties. Unlike the monomers, the polymers did not show any tendency for crystallization. In comparison to the monomers, the LC phase was stabilized in the polymers. Both the temperatures and the widths of the transitions were higher in the polymers. The DSC heating thermograms (Figure 7) for these polymers were characterized by T_g , above which the polymer changes over to the anisotropic fluid and the following endotherm was assigned for the anisotropic to isotropic transition. Similarly, in the cooling scan, an exotherm is seen for the isotropic to anisotropic phase change followed by a T_g , below which polymer chains lose their mobility and solidify retaining the anisotropic order. Figure 8 shows a microphotograph of PSCLCP-6, and Table 1 shows the transition temperatures of the homopolymers, PSCLCP- x . All the polymers exhibit a nematic mesophase. Similar to that of the monomers, the T_g of the polymers showed a decrease with increasing spacer length; however, no clear dependence of T_i on structure is observed.

The homopolymer of cholesteryl benzoate monomer, COP-0, showed a high transition temperature due to the bulky mesogenic group. The copolymers with different compositions also showed LC behavior, and both T_g and T_i increase with increasing cholesteric content (Table 2). When the transition temperature is above 200 °C

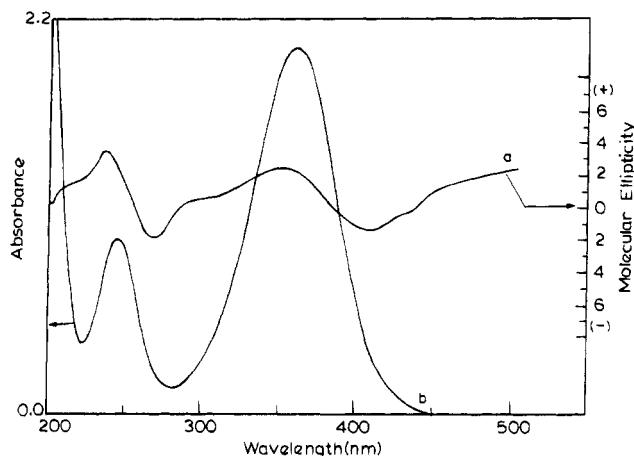


Figure 9. CD spectrum of COP-0 film containing 10 wt % of bis(benzylidene)cyclohexanone (a) and UV absorption spectrum of bis(benzylidene)cyclohexanone in chloroform (b).

for the copolymers, a partial thermal cross-linking (<10%) was observed and no clear transition peaks were seen after the first heating scan. The polymers containing the cholesteryl benzoate moiety were expected to show a cholesteric mesophase. However, this could not be confirmed from the textural information obtained by the POM studies. Induced circular dichroism (ICD) measurements were made to show the existence of the cholesteric mesophase.

It is well known that optical activity is induced in achiral species when they are dissolved in a cholesteric mesophase, giving rise to circular dichroism for the absorption bands of the achiral species. This phenomenon is called "liquid crystal induced circular dichroism (LCICD)".³⁸⁻⁴¹ The macroscopic helicoidal structure, known to exist in the cholesteric mesophase, is found to be essential for the observation of LCICD, since the transformation of the helical cholesteric structure to a uniaxial nematic mesophase by means of an electric field results in the loss of LCICD. A thin film of the homopolymer of cholesteryl benzoate doped with 10% by weight of an achiral bis(benzylidene)cyclohexanone was made by solution casting on a quartz plate and annealed for 15 min in the liquid crystalline state. The film was then used for the measurement of LCICD. Figure 9 shows the CD spectrum (curve a) of the film; the UV spectrum (curve b) for the dopant is also displayed for comparison. There are two positive peaks in the CD spectra with maxima near 242 and 350 nm, which coincides with the absorption maxima in the UV spectra, thus proving the cholesteric order in the polymer matrix.

In the copolymer systems there is no need to dope an achiral molecule, since the bis(benzylidene)cyclohexanone, present at the side chain, itself acts as the internal probe to measure the ICD. Figure 10 shows the CD spectra for COP-1 measured in the form of a film (curve a) as well as in solution (curve b). The appearance of ICD bands of the copolymer film at 260 and 360 nm shows the existence of spatial chirality. However, when the spectrum was recorded in solution, these two bands disappeared and a small band appeared near 240 nm. This is understandable because in solution there is no macroscopic helicoidal structure and hence no optical activity is induced into the achiral molecule. A small band near 240 nm is due to the molecular chirality of the cholesteric unit present in the polymer side chains. Curve c in Figure 10 is the CD spectrum of the PSCLCP-6 film. It shows no CD bands

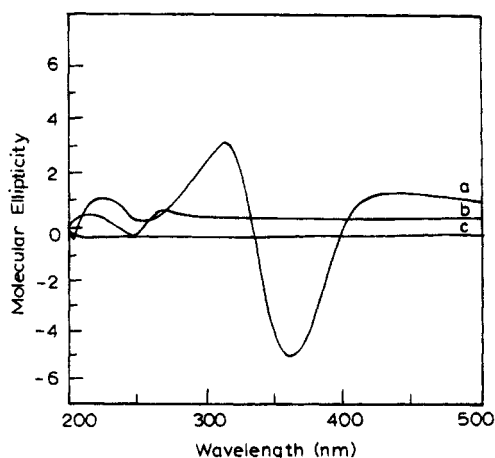


Figure 10. CD spectra of (a) COP-1 in film, (b) COP-1 in chloroform solution, and (c) PSCLCP-6 in film.

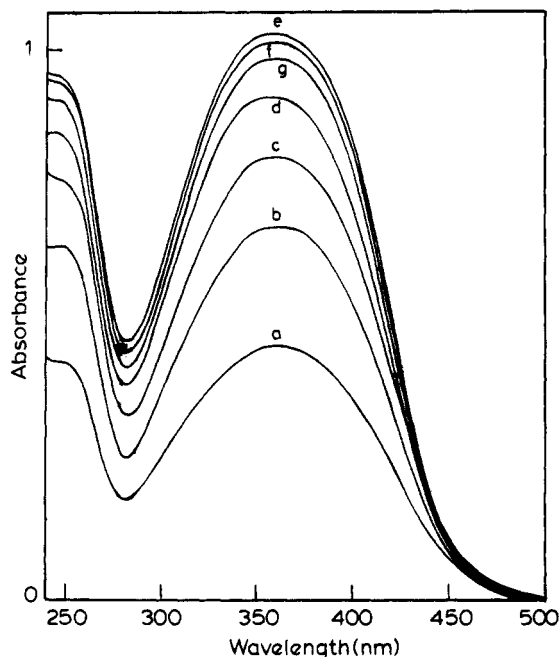


Figure 11. Changes in the UV spectral characteristics during the photolysis of OH-6 films at 80 °C for different time intervals: (a) 0, (b) 0.5, (c) 1, (d) 1.5, (e) 2, (f) 3, and (g) 4 min.

since the cholesteric units are absent in this polymer and hence does not exhibit the helicoidal supramolecular structure. These studies clearly demonstrate that cholesteryl benzoate groups incorporate the cholesteric mesomorphic behavior in the polymer. However, it should be noted that the CD spectral measurements were carried out at temperatures below T_g . Since these polymers freeze into a glassy state, with the retention of the LC order, it will be reasonable to assume that the same kind of order persists even in the LC state as well.

Photolysis Studies. The photochemical changes were followed by UV-visible and FTIR spectroscopic methods. Figure 11 shows the UV-visible spectral changes during the photoirradiation of OH-6 at 80 °C in the LC state. Before irradiation, the UV-visible spectrum shows an absorption maxima at 365 nm corresponding to the $\pi \rightarrow \pi^*$ transition of bis(benzylidene)cyclohexanone (curve a). After the first 0.5 min of irradiation, a sudden increase in the intensity of the peak maxima was observed, and this increase continued on further irradiation (curves b–e). After about 2 min,

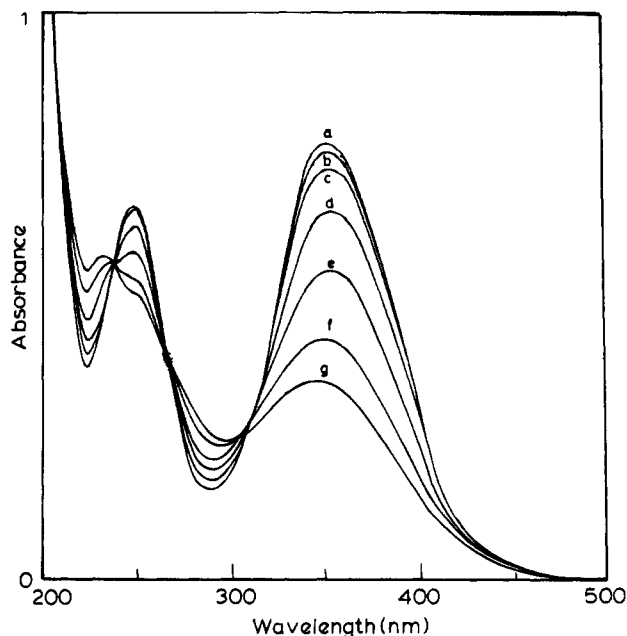


Figure 12. Changes in the UV spectral characteristics during the photolysis of PSCLCP-6 films at 120 °C for different time intervals: (a) 0, (b) 0.5, (c) 1, (d) 2, (e) 5, (f) 10, and (g) 15 min.

there was a reversal in the trend of intensity change, and thereafter a decrease in the intensity was observed (curves f and g). However, the magnitude of the intensity decrease at the later stages of photolysis is much smaller than that of the intensity increase at the initial part of the photolysis. The explanation for this kind of variation in intensity during photolysis could be obtained from our earlier studies.²² It has been shown that the increase of the UV-visible spectral peak intensity on irradiation is due to the disruption of the parallel aggregation of the mesogens in the LC state. The disruption of mesogenic order has been brought about by the *EZ* photoisomerization of the bis(benzylidene)cyclohexanone units. The resulting *EZ* isomer being nonlinear in shape not only introduces the disorder in the LC phase but also loses its mesogenic character. This explanation is supported by POM studies where a light-induced nematic to isotropic

transition is observed. Simultaneous irradiation and examination of the sample under polarized light revealed that the nematic texture disappears completely within a few minutes of irradiation and the sample melt changes from an anisotropic melt to an isotropic state at a constant temperature. The $2\pi + 2\pi$ addition reaction involves the consumption of C=C bonds, which is well reflected as a decrease in the intensity of the $\pi \rightarrow \pi^*$ transition at the later stages of photolysis.²² Since the quantum yield of the photoisomerization is higher than that of the $2\pi + 2\pi$ addition, one observes an increase in the intensity of the UV-visible absorption peaks at the initial stages of photolysis.

Figure 12 displays the UV-visible spectral changes during the photolysis of PSCLCP-6 in the LC state. A gradual decrease in the intensity of the 352 nm absorption band is observed, and after 15 min of irradiation, the film becomes completely insoluble, indicating the occurrence of cross-linking. Comparing the change in the UV-visible spectral pattern for OH-6 (Figure 11) and PSCLCP-6 (Figure 12) during photolysis, we find that there is no increase in the intensity at the initial stages in the latter case. The most plausible reason may be that the high melt viscosity of the polymer resists the disruption of the ordered arrangement of the chromophores. The extent of cross-linking was obtained by measuring the insoluble polymer after washing the irradiated film. The maximum extent of cross-linking was about 65% after 15 min of irradiation. The DSC thermogram of the cross-linked polymer did not show any peaks or baseline shift for the glass transition, indicating that the photo-cross-linking suppresses the thermal transitions in these polymers.

To understand more about the structural changes during the photo-cross-linking of the polymer, FTIR studies were carried out. Figure 13 shows the variation of the IR absorption bands with irradiation time. A regular decrease in the absorption of the C=C stretching band near 1600 cm^{-1} supports the fact that photo-cross-linking takes place at the exocyclic C=C of the bis(benzylidene)cyclohexanone. The decrease in the absorption of this band has been normalized with respect to that of the C=O absorption band and correlated to the rate of photo-cross-linking. Figure 14 shows the plot

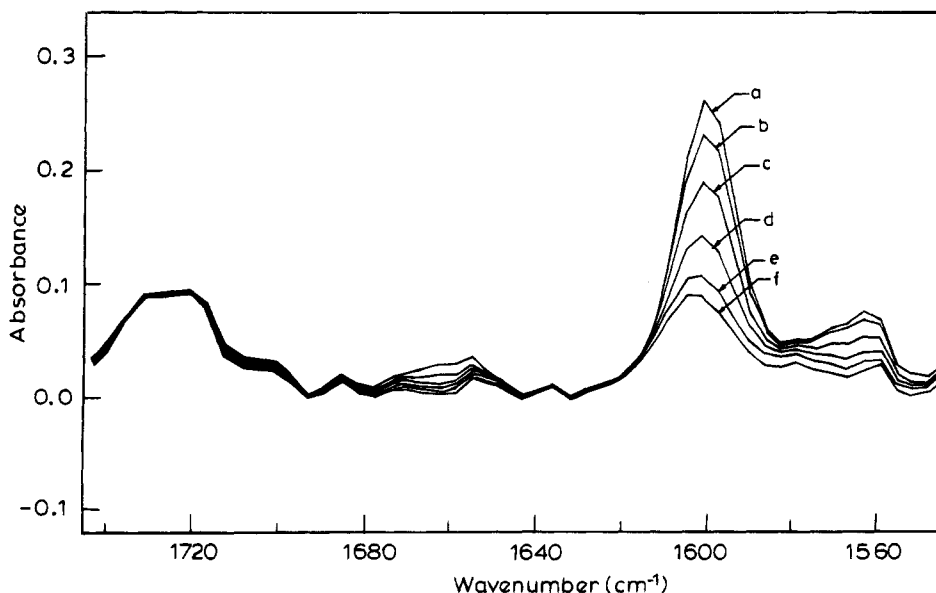


Figure 13. Changes in IR spectral characteristics of the PSCLCP-6 film on irradiation: (a) 0, (b) 0.5, (c) 1, (d) 3, (e) 10, and (f) 15 min.

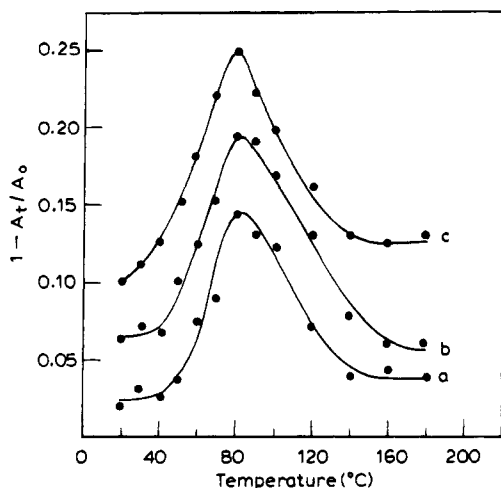


Figure 14. Temperature dependence of photochemical reactivity in PSCLCP-6 at different photolysis times: (a) 0.5, (b) 1, and (c) 2 min.

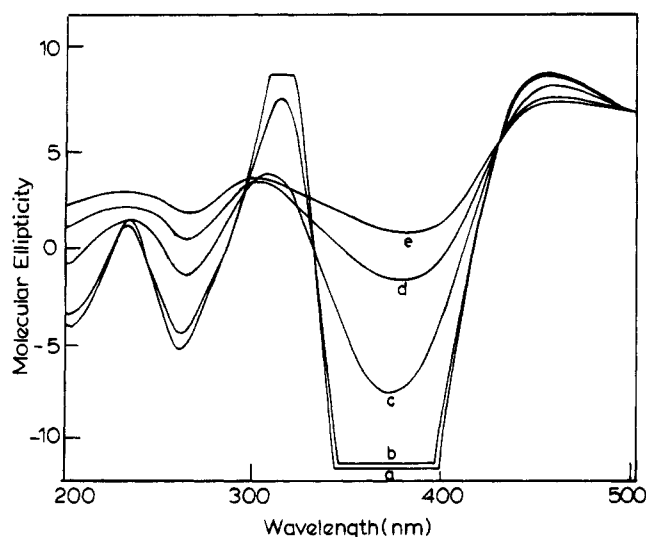


Figure 15. Change in CD spectral characteristics of the COP-4 film on irradiation: (a) 0 min; (b) 5 min; (c) 10 min; (d) 15 min; (e) after washing the cross-linked film with chloroform (here sensitivity has been increased by 50 times).

of $(A_t - A_0)/A_0$ versus temperature, where $A_t = A_{C=C}/A_{C=O}$ at time t , the ratio of the absorbance of the C=C stretching band to the absorbance for the C=O stretching band, and $A_t = A_0$ at $t = 0$. It can be seen from Figure 13 that there is a strong dependence of photo-reactivity on the temperature. The rate of photo-cross-linking increases with temperature in the vicinity of T_g and reaches a maximum at 80 °C, but above this temperature the trend changes and the rate decreases with increasing temperature.

The photo-cross-linking of the cholesteryl benzoate copolymer was studied by monitoring the ICD as a function of irradiation time. A thin film of the polymer was formed on a quartz plate and annealed in the LC phase for 15 min. The film was then cooled and used for measuring the CD spectra. Figure 15 shows the change in the spectra during the photolysis of COP-4. There is a regular decrease in the intensity with the irradiation time due to the consumption of the bis(benzylidene)cycloalkane groups, which act as the probe for the ICD (curves a–d). After 15 min of irradiation the cross-linked film was carefully washed with chloroform to remove the soluble part and dried. Curve e shows the CD spectrum for this film. The

appearance of the ICD bands, though of smaller intensity, confirms the fact that some degree of helicoidal structure remains intact even after the photo-cross-linking.

Conclusions

A new class of PSCLCPs containing the bis(benzylidene)cyclohexanone group has been synthesized, where the structure was varied with the spacer length. These variations have been correlated with the transition temperatures. The bis(benzylidene)cyclohexanone monomer has been copolymerized with the cholesteryl benzoate based monomer to incorporate cholesteric mesomorphism in the polymer. Irradiation of these copolymers gave cross-linked films with a helicoidal structure. Such films are attractive in passive electronic devices. The dual properties of the liquid crystallinity and photo-cross-linking of these polymers could be exploited in NLO applications. Poling in the LC phase facilitates easy orientation of the NLO molecules in an electric field,¹³ and photo-cross-linking of the poled film permanently freezes-in the orientation of the NLO molecules.^{42–44} This new class of polymers is devoid of any perceptible side reactions as compared to a similar class of polymers based on cinnamate esters. The *EZ* photoisomerization of bis(benzylidene)cycloalkane in the LC phase could be useful in developing optical information storage devices.^{45,46}

Acknowledgment. The authors thank Prof. N. V. Madhusudhana, Raman Research Institute, Bangalore, and Dr. V. Krishnamohan, INBRI, Bangalore, for their help in the POM and FTIR studies. This research was supported by the Department of Science and Technology, New Delhi.

References and Notes

- (1) *Recent Advances in Liquid Crystalline Polymers*; Chapoy, L. L., Ed.; Elsevier Applied Science: London, 1985.
- (2) *Side Chain Liquid Crystal Polymers*; McArdle, C. B., Ed.; Chapman and Hall: New York, 1989.
- (3) Noel, C.; Navard, P. *Prog. Polym. Sci.* **1991**, *16*, 55.
- (4) Ober, C. K.; Jin, J.-I.; Lenz, R. W. *Adv. Polym. Sci.* **1984**, *59*, 103.
- (5) Hani, R.; Lenz, R. W. *Silicon-Based Polymer Science: A Comprehensive Resource*; Advances in Chemistry 224; American Chemical Society: Washington, DC, 1990; p 741.
- (6) Creed, D.; Griffin, A. C.; Gross, J. R. D.; Hoyle, C. E.; Venkataram, K. *Mol. Cryst. Liq. Cryst.* **1988**, *155*, 57.
- (7) Ikeda, T.; Itakura, H.; Lee, C.; Winnik, F. M.; Tazuke, S. *Macromolecules* **1988**, *21*, 3537.
- (8) Keller, P. *Chem. Mater.* **1990**, *2*, 3.
- (9) Whitcombe, M. J.; Gilbert, A.; Hirai, A.; Mitchell, G. R. *J. Polym. Sci., Polym. Chem. Ed.* **1991**, *29*, 251.
- (10) Whitcombe, M. J.; Gilbert, A.; Mitchell, G. R. *Br. Polym. J.* **1990**, *23*, 77.
- (11) Griffin, A. C.; Hoyle, C. E.; Gross, J. R. D.; Venkataram, K.; Creed, D.; McArdle, C. B. *Makromol. Chem.* **1988**, *9*, 463.
- (12) Legge, C. H.; Whitcombe, M. J.; Gilbert, A.; Mitchell, G. R. *J. Mater. Chem.* **1991**, *1*, 303.
- (13) Mohlmann, G. R.; van der Vorst, C. P. J. M. *Side Chain Liquid Crystal Polymers*; McArdle, C. B., Ed.; Chapman and Hall: New York, 1989; p 330.
- (14) Marturunkakul, S.; Chen, I. J.; Li, L.; Jeng, R. J.; Kumar, J.; Tripathy, S. K. *Chem. Mater.* **1993**, *5*, 592.
- (15) Koch, T.; Ritter, H.; Buchholz, N. *Makromol. Chem.* **1989**, *190*, 1369.
- (16) Loth, H.; Euschem, A. *Makromol. Chem., Rapid Commun.* **1988**, *9*, 35.
- (17) Creed, D.; Griffin, A. C.; Hoyle, C. E.; Venkataram, K. *J. Am. Chem. Soc.* **1990**, *112*, 4049.
- (18) Noonan, J. M.; Caccamo, A. F. *Polym. Prepr. (Am. Chem. Soc., Div. Polym. Chem.)* **1984**, *30*, 501.
- (19) Krigbaum, W. R.; Ishikawa, T.; Watanabe, J.; Toriumi, H.; Kubota, K. *J. Polym. Sci., Polym. Chem. Ed.* **1983**, *21*, 1851.

- (20) Peter, K.; Ratzsch, M. *Makromol. Chem.* **1990**, *191*, 1021.
(21) Whitcombe, M. J.; Gilbert, A.; Mitchell, G. R. *J. Polym. Sci., Polym. Chem. Ed.* **1992**, *30*, 1681.
(22) Gangadhara; Kishore, K. *Macromolecules* **1993**, *26*, 2995.
(23) McArdle, C. B. *Side Chain Liquid Crystal Polymers*; McArdle, C. B., Ed.; Chapman and Hall: New York, 1989; p 1.
(24) George, H.; Roth, H. T. *Tetrahedron Lett.* **1971**, *43*, 4057.
(25) Wagnier, F. B.; Feigenbaum, A.; Muzart, J. *J. Chem. Educ.* **1978**, *55*, 339.
(26) Forward, G. C.; Whiting, D. A. *J. Chem. Soc. C* **1969**, 1868.
(27) Frey, H.; Behmann, G.; Kaupp, G. *Chem. Ber.* **1987**, *120*, 387.
(28) Kaupp, G.; Zimmermann, I. *Angew. Chem., Int. Ed. Engl.* **1981**, *20*, 1018.
(29) Theocharis, C. R.; Jones, W.; Thomas, M. J.; Molevalli, M.; Hursthouse, B. M. *J. Chem. Soc., Perkin Trans. 2* **1984**, 71.
(30) Aizeshtat, Z.; Hausmann, M.; Pickholtz, Y.; Tal, D.; Blum, J. *J. Org. Chem.* **1977**, *42*, 2386.
(31) Broer, D. J.; Heynderickx, I. *Macromolecules* **1990**, *23*, 2474.
(32) Heynderickx, I.; Broer, D. J. *Mol. Cryst. Liq. Cryst.* **1991**, *203*, 113.
(33) Hikmet, R. A. M.; Lub, J.; Broer, D. J. *Adv. Mater.* **1991**, *23*, 113.
(34) Vedejs, E.; Arnost, M. J.; Hagan, J. P. *J. Org. Chem.* **1979**, *44*, 3230.
(35) Kang, S-Ku.; Kim, W-Sup.; Moon, B-Ho. *Synthesis* **1985**, *12*, 1161.
(36) Cheng, S. Z. D. *Macromolecules* **1988**, *21*, 2475.
(37) Cheng, S. Z. D.; Zhang, A.; Johnson, R. L.; Zhou, Z. *Macromolecules* **1989**, *22*, 4292.
(38) Saeva, F. D.; Wysocki, J. J. *J. Am. Chem. Soc.* **1971**, *93*, 5928.
(39) Saeva, F. D. *Mol. Cryst. Liq. Cryst.* **1972**, *18*, 375.
(40) Saeve, F. D. *J. Am. Chem. Soc.* **1972**, *94*, 5135.
(41) Saeve, F. D.; Sharpe, P. E.; Olin, G. R. *J. Am. Chem. Soc.* **1973**, *95*, 7956.
(42) Mandal, B. K.; Kumar, J.; Huang, J. C.; Tripathy, S. *Makromol. Chem., Rapid Commun.* **1991**, *12*, 63.
(43) Mandal, B. K.; Jeng, R. J.; Kumar, J.; Tripathy, S. *Makromol. Chem., Rapid Commun.* **1991**, *12*, 607.
(44) Chen, M.; Yu, L.; Dalton, L. R.; Shi, Y.; Steier, W. H. *Macromolecules* **1991**, *24*, 5421.
(45) George, A.; Corrie, I. *New Scientist* **1991**, 1768, 39.
(46) McArdle, C. B. *Side Chain Liquid Crystal Polymers*; McArdle, C. B., Ed.; Chapman and Hall: New York, 1989; p 375.

MA9410734